

Comparison of Accuracy and Scalability of Gauss-Newton and Alternating Least Squares for CP Decomposition

Navjot Singh*, Linjian Ma[†], Hongru Yang[†], and Edgar Solomonik[†]

**Department of Mathematics*

†Department of Computer Science

University of Illinois at Urbana-Champaign, Urbana, IL

{navjot2, lma16, hyang87, solomon2}@illinois.edu

Abstract—Alternating least squares is the most widely used algorithm for CP tensor decomposition. However, alternating least squares may exhibit slow or no convergence, especially when high accuracy is required. An alternative approach is to regard CP decomposition as a nonlinear least squares problem and employ Newton-like methods. Direct solution of linear systems involving an approximated Hessian is generally expensive. However, recent advancements have shown that use of an implicit representation of the linear system makes these methods competitive with alternating least squares. We provide the first parallel implementation of a Gauss-Newton method for CP decomposition, which iteratively solves linear least squares problems at each Gauss-Newton step. In particular, we leverage a formulation that employs tensor contractions for implicit matrix-vector products within the conjugate gradient method. The use of tensor contractions enables us to employ the Cyclops library for distributed-memory tensor computations to parallelize the Gauss-Newton approach with a high-level Python implementation. We study the convergence of variants of the Gauss-Newton method relative to ALS for finding exact CP decompositions as well as approximate decompositions of real-world tensors. We evaluate the performance of both sequential and parallel versions of both approaches, and study the parallel scalability on the Stampede2 supercomputer.

Index Terms—tensor decomposition, alternating least squares, Gauss-Newton method, CP decomposition, Cyclops Tensor Framework

I. INTRODUCTION

The CP (canonical polyadic or CANDECOMC/PARAFAC) tensor decomposition is widely used for data analytics in different scientific fields [11], [15], [23], [27], [36], machine learning applications [2], [4], [20], and quantum chemistry [43]. CP decomposition of an input tensor can be computed via different optimization techniques, such as variants of gradient descent [1], [30], deflations [2], [3], and alternating least squares [20].

Nowadays, the alternating least squares (ALS) method, which solves quadratic optimization subproblems for each factor matrix in an alternating manner, is most commonly used and has become a target for parallelization [14], [18], performance optimization [22], [35], and acceleration by randomization [8]. A major advantage of ALS is its guar-

anteed monotonic decrease of the residual. However, there are many cases where ALS shows slow or no convergence when solution with high resolution is required, which is also called the ‘swamp’ phenomenon [24]. Swamps deteriorate both the running time and the convergence behavior of the ALS method. Consequently, researchers have been looking at different alternatives to ALS, including various regularization techniques [21], [28], line search [25], [29], [34] and gradient based methods [1], [30], [33], [40], [44], [46].

Of the variants of gradient based methods, one promising approach is to perform the CP decomposition by solving a nonlinear least squares problem using the Newton or Gauss-Newton methods [30], [45], [46]. These approaches offer quadratic convergence and are better at avoiding the swamps inhibiting performance of ALS. Naive solution of linear equations arising in these method is expensive. For rank- R decomposition of an N dimensional tensor with all the dimension sizes equal to s , standard algorithms either perform Cholesky on the normal equations [30] or QR on the Jacobian matrix [46], yielding a complexity of $O(N^3 s^3 R^3)$. However, the matrices involved in this linear system are sparse and have much implicit structure. A recent advancement has shown that the cost of inverting the Hessian can be reduced to $O(N^3 R^6)$ [33]. A successive study showed that the cost can be further reduced to $O(NR^6)$, albeit the approach can suffer from numerical instability [44].

Another approach for performing Gauss-Newton with low cost is to leverage an implicit conjugate gradient (CG) method [40]. The structure of the approximated Hessian can be leveraged to perform fast matrix-vector multiplications for CG iterations (with a cost of $O(N^2 s R^2)$ per iteration), an approach that can also be augmented with preconditioning to accelerate CG convergence rate [40]. In comparison to the aforementioned direct methods, this iterative approach is substantially more scalable with respect to the CP rank R . This advantage is critical in many applications of CP decomposition, as in many cases $R \geq s$ is needed (in general CP rank can be as high as s^{N-1} for an order N tensor). Moreover, for the CP decomposition with rank $R < s$,

Tucker decomposition (or simply HoSVD) [48] can be used to effectively compress the input tensor from dimensions of size s to R , and then CP decomposition can be performed.

In this paper, we investigate the behavior of Gauss-Newton optimization with preconditioned CG on CP decomposition in high rank scenarios (with $R \geq s$ or more generally when the rank is at least the smallest dimension size of the input tensor). We consider various approaches to regularization for both ALS and Gauss-Newton with implicit CG. To understand their efficacy, we quantify their ability to converge to exact CP decompositions of synthetic tensor of various CP rank, as well as to approximating tensors arising in applications in quantum chemistry. With the best regularization strategy, we find that Gauss-Newton is able to consistently find exact CP decompositions for problems where ALS generally does not converge. Further, the Gauss-Newton method obtains lower residuals in approximation. We present these results in Section V.

Our main contribution is the parallel implementation of Gauss-Newton with implicit CG, via a tensor-contraction-based formulation of the method. We develop a distributed-memory implementation of the method using the Cyclops library for parallel tensor algebra. Our implementation interpolates between a sequential approach based on the NumPy library and the Cyclops backend, enabling both sequential and parallel experimental studies. We detail our implementations in Section IV. We evaluate the strong and weak scalability of the method on the Stampede2 supercomputer, and compare its performance to ALS for a variety of test problems. Our results demonstrate that the Gauss-Newton method can converge faster both in sequential and parallel settings. These results are presented in Section V-C,V-D.

This paper makes the following contributions:

- We cast the large matrix-vector multiplication into several tensor contractions so that an existing library on parallel tensor contractions can be utilized. Our analysis achieves the same computational cost as previous work [40].
- We propose and evaluate a new regularization strategy, and demonstrate that it is well-suited for CP decomposition with Gauss-Newton.
- We provide the first parallel implementation of Gauss-Newton for CP decomposition.
- We demonstrate that an implementation of parallel Gauss-Newton with preconditioned CG can both converge faster and achieve higher convergence probability for CP decomposition of both synthetic and application-based tensors.

II. BACKGROUND

A. Notation and Definitions

We use tensor algebra notation in both element-wise form and specialized form for tensor operations [20]. For vectors, bold lowercase Roman letters are used, e.g., \mathbf{x} . For matrices, bold uppercase Roman letters are used, e.g., \mathbf{X} . For tensors, bold calligraphic fonts are used, e.g., \mathcal{X} . An order N tensor corresponds to an N -dimensional array with dimensions

$s_1 \times \cdots \times s_N$. Elements of vectors, matrices, and tensors are denoted in subscript, e.g., x_i for a vector \mathbf{x} , x_{ij} for a matrix \mathbf{X} , and x_{ijkl} for an order 4 tensor \mathcal{X} . The i th column of a matrix \mathbf{X} is denoted by \mathbf{x}_i . The mode- n matrix product of a tensor $\mathcal{X} \in \mathbb{R}^{s_1 \times \cdots \times s_N}$ with a matrix $\mathbf{A} \in \mathbb{R}^{J \times s_n}$ is denoted by $\mathcal{X} \times_n \mathbf{A}$, with the result having dimensions $s_1 \times \cdots \times s_{n-1} \times J \times s_{n+1} \times \cdots \times s_N$. Matricization is the process of reshaping a tensor into a matrix. Given a tensor \mathcal{X} the mode- n matricized version is denoted by $\mathbf{X}_{(n)} \in \mathbb{R}^{s_n \times K}$ where $K = \prod_{m=1, m \neq n}^N s_m$. We use parenthesized superscripts as labels for different tensors and matrices, e.g., $\mathbf{A}^{(1)}$ and $\mathbf{A}^{(2)}$ are different matrices.

The Hadamard product of two matrices $\mathbf{U}, \mathbf{V} \in \mathbb{R}^{I \times J}$ resulting in matrix $\mathbf{W} \in \mathbb{R}^{I \times J}$ is denoted by $\mathbf{W} = \mathbf{U} * \mathbf{V}$, where $w_{ij} = u_{ij}v_{ij}$. The inner product of matrices \mathbf{U}, \mathbf{V} is denoted by $\langle \mathbf{U}, \mathbf{V} \rangle = \sum_{i,j} u_{ij}v_{ij}$. The outer product of K vectors $\mathbf{u}^{(1)}, \dots, \mathbf{u}^{(K)}$ of corresponding sizes s_1, \dots, s_K is denoted by $\mathcal{X} = \mathbf{u}^{(1)} \circ \cdots \circ \mathbf{u}^{(K)}$ where $\mathcal{X} \in \mathbb{R}^{s_1 \times \cdots \times s_K}$ is an order K tensor. For matrices $\mathbf{A} \in \mathbb{R}^{I \times K} = [\mathbf{a}_1, \dots, \mathbf{a}_K]$ and $\mathbf{B} \in \mathbb{R}^{J \times K} = [\mathbf{b}_1, \dots, \mathbf{b}_K]$, their Khatri-Rao product resulting in a matrix of size $(IJ) \times K$ defined by $\mathbf{A} \odot \mathbf{B} = [\mathbf{a}_1 \otimes \mathbf{b}_1, \dots, \mathbf{a}_K \otimes \mathbf{b}_K]$, where $\mathbf{a} \otimes \mathbf{b}$ denotes the Kronecker product of the two vectors.

B. CP Decomposition with Alternating Least Squares

The CP tensor decomposition [13], [15] is denoted by

$$\mathcal{X} \approx [\mathbf{A}^{(1)}, \dots, \mathbf{A}^{(N)}], \quad \text{where } \mathbf{A}^{(i)} = [\mathbf{a}_1^{(i)}, \dots, \mathbf{a}_r^{(i)}],$$

and serves to approximate a tensor by a sum of R tensor products of vectors,

$$\mathcal{X} \approx \sum_{r=1}^R \mathbf{a}_r^{(1)} \circ \cdots \circ \mathbf{a}_r^{(N)}.$$

The CP-ALS method alternates among quadratic optimization problems for each of the factor matrices $\mathbf{A}^{(n)}$, resulting in linear least squares problems for each row,

$$\mathbf{A}_{\text{new}}^{(n)} \mathbf{P}^{(n)T} \cong \mathbf{X}_{(n)},$$

where the matrix $\mathbf{P}^{(n)} \in \mathbb{R}^{I_n \times R}$, where $I_n = s_1 \times \cdots \times s_{n-1} \times s_{n+1} \times \cdots \times s_N$ is formed by Khatri-Rao products of the other factor matrices,

$$\mathbf{P}^{(n)} = \mathbf{A}^{(1)} \odot \cdots \odot \mathbf{A}^{(n-1)} \odot \mathbf{A}^{(n+1)} \odot \cdots \odot \mathbf{A}^{(N)}. \quad (1)$$

These linear least squares problems are often solved via the normal equations [20]:

$$\mathbf{A}_{\text{new}}^{(n)} \mathbf{\Gamma}^{(n)} \leftarrow \mathbf{X}_{(n)} \mathbf{P}^{(n)},$$

where $\mathbf{\Gamma} \in \mathbb{R}^{r \times r}$ can be computed via

$$\mathbf{\Gamma}^{(n)} = \mathbf{S}^{(1)} * \cdots * \mathbf{S}^{(n-1)} * \mathbf{S}^{(n+1)} * \cdots * \mathbf{S}^{(N)}, \quad (2)$$

with each $\mathbf{S}^{(i)} = \mathbf{A}^{(i)T} \mathbf{A}^{(i)}$. These equations also give the n th component of the optimality conditions for the unconstrained minimization of the nonlinear objective function,

$$f(\mathbf{A}^{(1)}, \dots, \mathbf{A}^{(N)}) := \frac{1}{2} \|\mathcal{X} - [\mathbf{A}^{(1)}, \dots, \mathbf{A}^{(N)}]\|_F^2. \quad (3)$$

The *Matricized Tensor Times Khatri-Rao Product* or MTTKRP computation $\mathbf{M}^{(n)} = \mathbf{X}_{(n)}\mathbf{P}^{(n)}$ is the main computational bottleneck of CP-ALS [7]. Within MTTKRP, the bottleneck is the contraction between the input tensor and the first-contracted matrix, and we call this step *first contraction* of the MTTKRP. Algebraically, this contraction can be written as the tensor times matrix product, $\mathcal{X} \times_i \mathbf{A}^{(i)T}$. For a rank- R CP decomposition, this computation has the cost of $2s^N R$ if $s_n = s$ for all $n \in \{1, \dots, N\}$.

The dimension-tree algorithm for ALS [6], [19], [32], [49] uses a fixed amortization scheme to update MTTKRP in each ALS sweep. This scheme only needs to perform two first contraction calculations for each ALS sweep, decreasing the leading order cost of a sweep from $2Ns^N R$ to $4s^N R$.

III. GAUSS-NEWTON FOR CP DECOMPOSITION

The Gauss-Newton (GN) method is a modification of the Newton's method to solve non-linear least squares problem for a quadratic objective function defined as

$$\phi(\mathbf{x}) = \frac{1}{2} \|\mathbf{y} - \mathbf{f}(\mathbf{x})\|^2,$$

where \mathbf{y} is the given vector of points with respect to which we solve the least squares problem, \mathbf{x} is the solution vector required and \mathbf{f} is the non-linear function of \mathbf{x} given in the problem. The gradient and the Hessian matrix of $\phi(\mathbf{x})$ can be expressed as

$$\begin{aligned} \nabla \phi(\mathbf{x}) &= \mathbf{J}_r^T(\mathbf{x})\mathbf{r}(\mathbf{x}), \\ \mathbf{H}_\phi(\mathbf{x}) &= \mathbf{J}_r^T(\mathbf{x})\mathbf{J}_r(\mathbf{x}) + \sum_i r_i(\mathbf{x})\mathbf{H}_{r_i}(\mathbf{x}), \end{aligned}$$

where $\mathbf{r}(\mathbf{x})$ is the residual function defined as $\mathbf{r}(\mathbf{x}) = \mathbf{y} - \mathbf{f}(\mathbf{x})$, $\mathbf{J}_r(\mathbf{x})$ is the Jacobian matrix of the residual function with respect to \mathbf{x} , and $\mathbf{H}_{r_i}(\mathbf{x})$ is the Hessian matrix of the residual function r_i with respect to \mathbf{x} .

The Gauss-Newton method leverages the fact that $\mathbf{H}_{r_i}(\mathbf{x})$ is small in norm when the residual is small, to approximate the Hessian as $\mathbf{H}_\phi(\mathbf{x}) \approx \mathbf{J}_r^T(\mathbf{x})\mathbf{J}_r(\mathbf{x})$. Consequently, the Gauss-Newton iteration aims to perform the update,

$$\mathbf{x}^{(k+1)} = \mathbf{x}^{(k)} - (\mathbf{J}_r^T(\mathbf{x}^{(k)})\mathbf{J}_r(\mathbf{x}^{(k)}))^{-1} \mathbf{J}_r^T(\mathbf{x}^{(k)})\mathbf{r}(\mathbf{x}^{(k)}),$$

where $\mathbf{x}^{(k)}$ represents the \mathbf{x} at k th iteration. This linear system corresponds to the normal equations for the linear least squares problem,

$$\mathbf{J}_r(\mathbf{x}^{(k)})(\mathbf{x}^{(k+1)} - \mathbf{x}^{(k)}) \cong -\mathbf{r}(\mathbf{x}^{(k)}).$$

The CP decomposition can be formulated as a non-linear least square problem in (3).

We define the Jacobian tensor as

$$\mathcal{J} = [\mathcal{J}^{(1)}, \dots, \mathcal{J}^{(N)}]$$

for the N -dimensional CP decomposition, where $\mathcal{J}^{(n)} \in \mathbb{R}^{s_1 \times \dots \times s_N \times s_n \times R}$ is the Jacobian tensor for the residual tensor with respect to $\mathbf{A}^{(n)}$, and is expressed element-wise as

$$\dot{j}_{i_1 \dots i_N k r}^{(n)} = \left(- \prod_{m=1, m \neq n}^N a_{i_m r}^{(m)} \right) \delta_{i_n k}. \quad (4)$$

Another way to derive the Jacobian matrices is by unfolding the factor matrices and the residual function as suggested in [1]. Factorization of the Hessian to solve a linear system in Gauss-Newton has cost $O(N^3 s^3 R^3)$. More advanced approaches to solving Hessian can achieve a cost of $O(NR^6)$ [44], but this reduction is not substantial when CP rank is high, i.e., $R \geq s$.

Alternatively, conjugate gradient (CG) with implicit matrix products can be used to solve the linear least squares problems in this Gauss-Newton method [40]. Instead of performing a factorization or inversion of the approximate Hessian matrix, this approach needs only to perform matrix vector products $\mathbf{J}^T \mathbf{J} \mathbf{v}$ at each iteration (henceforth we drop the subscript r from \mathbf{J}_r and simply refer to \mathbf{J} for the matrix form of the Jacobian and \mathcal{J} for its tensor form). We derive the matrix vector product in terms of tensor contractions in the following section.

A. Gauss-Newton with Implicit Conjugate Gradient

With the Jacobian tensors defined in (4), the matrix-matrix product $\mathbf{H} = \mathbf{J}^T \mathbf{J}$ can be expressed as an operator with the following form,

$$h_{krlz}^{(n,p)} = \sum_{i_1 \dots i_N} \dot{j}_{i_1 \dots i_N k r}^{(n)} \dot{j}_{i_1 \dots i_N l z}^{(p)},$$

which can be simplified to

$$h_{krlz}^{(n,p)} = \begin{cases} \delta_{kl} \Gamma_{rz}^{(n,n)}, & \text{if } n = p \\ a_{kz}^{(n)} a_{lr}^{(p)} \Gamma_{rz}^{(n,p)}, & \text{otherwise} \end{cases}, \quad (5)$$

$$\text{where } \Gamma_{rz}^{(n,p)} = \prod_{m=1, m \neq n, p}^N \left(\sum_{i_m} a_{i_m r}^{(m)} a_{i_m z}^{(m)} \right). \quad (6)$$

Note that $\Gamma^{(n,n)} = \Gamma^{(n)}$ as defined in (2). The matrix-vector product $\mathbf{H} \mathbf{w}$ can be written as

$$\mathbf{H} \mathbf{w} = \sum_{n=1}^N \sum_{p=1}^N \sum_{l=1}^{s_p} \sum_{z=1}^R h_{krlz}^{(n,p)} w_{lz}^{(p)}.$$

The contractions in the innermost summation have the form,

$$\sum_{l,z} h_{krlz}^{(n,p)} w_{lz}^{(p)} = \begin{cases} \sum_z \Gamma_{rz}^{(n,n)} w_{kz}^{(n)}, & \text{if } n = p, \\ \sum_{l,z} a_{kz}^{(n)} a_{lr}^{(p)} \Gamma_{rz}^{(n,p)} w_{lz}^{(p)} & \text{otherwise.} \end{cases} \quad (7)$$

Computation of $\sum_{n=1}^N \sum_{p=1}^N \sum_{l,z} h_{krlz}^{(n,p)} w_{lz}^{(p)}$ requires N^2 contractions of the form $\sum_{l,z} h_{krlz}^{(n,p)} w_{lz}^{(p)}$ for a total cost of $O(N^2 s R^2)$

when each mode of the input tensor has size s and is $O\left(N \left(\sum_{m=1}^N s_m \right) R^2\right)$ in the general case. Our Gauss-Newton algorithm is summarized in Algorithm 1.

Algorithm 1 CP-GN: Gauss-Newton with preconditioned implicit CG for CP decomposition

```

1: Input: Tensor  $\mathcal{X} \in \mathbb{R}^{s_1 \times \dots \times s_N}$ , stopping criteria  $\varepsilon$ , CG stopping criteria  $\varepsilon_{cg}$ , rank  $R$ 
2: Initialize  $\{\mathbf{A}^{(1)}, \dots, \mathbf{A}^{(N)}\}$  so each  $\mathbf{A}^{(n)} \in \mathbb{R}^{s_n \times R}$  is random
3: while  $\sum_{i=1}^N \|\mathbf{G}^{(i)}\|_F > \varepsilon$  do
     $\triangleright$  Using dimension tree with  $\mathbf{P}^{(n)}$  is defined as in (1)
4:   Calculate  $\mathbf{M}^{(n)} = \mathbf{X}_{(n)} \mathbf{P}^{(n)}$  for  $n \in \{1, \dots, N\}$ 
5:   for  $n \in \{1, \dots, N\}$  do
6:     Calculate  $\mathbf{\Gamma}^{(n,p)}$  for  $p \in \{1, \dots, N\}$  based on (6)
7:      $\mathbf{G}^{(n)} \leftarrow \mathbf{A}^{(n)} \mathbf{\Gamma}^{(n,n)} - \mathbf{M}^{(n)}$ 
8:   end for
9:   Define  $\lambda$  based on varying scheme described in Section III-B
      $\{\mathbf{V}^{(1)}, \dots, \mathbf{V}^{(N)}\} \leftarrow \text{CP-CG}(\mathcal{X}, \{\mathbf{G}^{(1)}, \dots, \mathbf{G}^{(N)}\},$ 
        $\{\mathbf{A}^{(1)}, \dots, \mathbf{A}^{(N)}\},$ 
        $\{\mathbf{\Gamma}^{(n,p)} : n, p \in \{1, \dots, N\}\},$ 
        $\varepsilon_{cg}, \lambda)$ 
10:
11:   for  $n \in \{1, \dots, N\}$  do
12:      $\mathbf{A}^{(n)} \leftarrow \mathbf{A}^{(n)} + \mathbf{V}^{(n)}$ 
13:   end for
14: end while
15: return factor matrices  $\{\mathbf{A}^{(1)}, \dots, \mathbf{A}^{(N)}\}$  with  $\mathbf{A}^{(n)} \in \mathbb{R}^{s_n \times R}$ 

```

B. Regularization for Gauss-Newton

Since the approximated Hessian is inherently rank-deficient [46], we incorporate Tikhonov regularization when solving the linear system, $\mathbf{J}^T \mathbf{J} + \lambda \mathbf{I}$, at each iteration, which corresponds to the Levenberg-Marquardt algorithm [26]. The convergence behavior of the Gauss-Newton method for CP decomposition as well as the CG method used within each Gauss-Newton iteration is sensitive to the choice of regularization parameter.

A common approach to resolve the scaling indeterminacy for the linear least squares problem is to use $\mathbf{J}^T \mathbf{J} + \lambda \text{diag}(\mathbf{J}^T \mathbf{J})$, however, this hinders the ability of the Gauss-Newton method to achieve second order convergence [26]. There are several other approaches for choosing the damping parameter and the diagonal matrix at each iteration to ensure local convergence of the algorithm [26], but those are costly in the context of CP decomposition, due to the computational expense associated with each iteration.

We provide a new heuristic approach for choosing the damping parameter with identity diagonal matrix by varying the regularization at each step. Variable regularization has been used in the past for the Gauss-Newton method, by increasing or decreasing the parameter depending on the value of the objective function at the next iteration [26]. We find that for CP decomposition, variation of the regularization parameter is useful for getting out of swamps, and adjusting it eagerly helps avoid the need for expensive recomputation of the objective.

In particular, we define an upper threshold and a lower threshold, and initialize λ near the upper threshold. This larger value ensures that we take steps towards the negative gradient direction, and enables CG to converge quickly. Next, we choose a constant hyper parameter $\mu > 1$ and update the λ at each iteration with $\lambda = \lambda/\mu$. This update is continued until λ reaches the lower threshold, and then it is increased by the

Algorithm 2 CP-CG: Preconditioned implicit CG for CP decomposition

```

1: Input: Tensor  $\mathcal{X} \in \mathbb{R}^{s_1 \times \dots \times s_N}$ , gradient set  $\{\mathbf{G}^{(1)}, \dots, \mathbf{G}^{(N)}\}$ , factor matrix set  $\{\mathbf{A}^{(1)}, \dots, \mathbf{A}^{(N)}\}$ , set of  $R \times R$  matrices  $\{\mathbf{\Gamma}^{(n,p)} : n, p \in \{1, \dots, N\}\}$ , stopping criteria  $\varepsilon_{cg}$ , regularization term  $\lambda$ 
2: for  $n \in \{1, \dots, N\}$  do
3:    $\mathbf{P}_{\text{inv}}^{(n)} \leftarrow (\mathbf{\Gamma}^{(n,n)} + \lambda \mathbf{I})^{-1}$ 
4:   Initialize  $\mathbf{V}^{(n)}$  to zeros
5:    $\mathbf{R}^{(n)} \leftarrow -\mathbf{G}^{(n)}$ 
6:    $\mathbf{Z}^{(n)} \leftarrow \mathbf{R}^{(n)} \mathbf{P}_{\text{inv}}^{(n)}$ 
7:    $\mathbf{W}^{(n)} \leftarrow \mathbf{Z}^{(n)}$ 
8: end for
9: while  $\sum_{i=1}^N \|\mathbf{R}^{(i)}\|_F > \varepsilon_{cg} \sum_{i=1}^N \|\mathbf{G}^{(i)}\|_F$  do
10:  for  $n \in \{1, \dots, N\}$  do
     $\triangleright$  Using implicit matrix vector product as in (7)
11:     $\mathbf{Q}^{(n)} \leftarrow \lambda \mathbf{W}^{(n)} + \sum_{p=1}^N \text{MatVec}(\mathbf{A}^{(n)}, \mathbf{A}^{(p)}, \mathbf{\Gamma}^{(n,p)}, \mathbf{W}^{(p)})$ 
12:    end for
13:     $\alpha \leftarrow \sum_{n=1}^N \langle \mathbf{R}^{(n)}, \mathbf{Z}^{(n)} \rangle / \sum_{n=1}^N \langle \mathbf{W}^{(n)}, \mathbf{Q}^{(n)} \rangle$ 
14:    for  $n \in \{1, \dots, N\}$  do
15:       $\mathbf{V}^{(n)} \leftarrow \mathbf{V}^{(n)} + \alpha \mathbf{W}^{(n)}$ 
16:       $\mathbf{R}^{(n)} \leftarrow \mathbf{R}^{(n)} - \alpha \mathbf{Q}^{(n)}$ 
17:       $\mathbf{Z}^{(n)} \leftarrow \mathbf{R}^{(n)} \mathbf{P}_{\text{inv}}^{(n)}$ 
18:    end for
19:     $\beta \leftarrow \sum_{n=1}^N \langle \mathbf{R}^{(n)}, \mathbf{Z}^{(n)} \rangle / \sum_{n=1}^N \langle \mathbf{W}^{(n)}, \mathbf{Q}^{(n)} \rangle$ 
20:    for  $n \in \{1, \dots, N\}$  do
21:       $\mathbf{W}^{(n)} \leftarrow \mathbf{Z}^{(n)} + \beta \mathbf{W}^{(n)}$ 
22:    end for
23:  end while
24: return updates to factor matrices  $\{\mathbf{V}^{(1)}, \dots, \mathbf{V}^{(N)}\}$ 

```

update $\lambda = \lambda\mu$ until it reaches the upper threshold value and then decreased again. The lower threshold ensures that the conditioning of $\mathbf{J}^T \mathbf{J}$ does not affect the CG updates.

We show in Section V-A that this type of varying regularization can significantly improve the convergence probability of Gauss-Newton method relative to a fixed regularization parameter when an exact CP decomposition exists. We find that this strategy is robust in speed and convergence probability across many experiments.

C. Preconditioning for Conjugate Gradient

Preconditioning is often used to reduce the number of iterations in conjugate gradient. For CP decomposition, the structure of the Gauss-Newton approximate Hessian $\mathbf{H} = \mathbf{J}^T \mathbf{J}$ admits a natural block-diagonal Kronecker product preconditioner [33]. Each of the N diagonal blocks $\mathbf{H}^{(n,n)}$ has a Kronecker product structure, $\mathbf{H}^{(n,n)} = \mathbf{\Gamma}^{(n,n)} \otimes \mathbf{I}$. Consequently, its inverse is

$$\mathbf{H}^{(n,n)^{-1}} = \mathbf{\Gamma}^{(n,n)^{-1}} \otimes \mathbf{I},$$

which can be computed using $O(R^3)$ work per Gauss-Newton iteration and applied with $O(sR^2)$ cost per CG iteration.

We can also use the Cholesky factorization $\mathbf{\Gamma}^{(n,n)} = \mathbf{L}\mathbf{L}^T$,

$$\mathbf{H}^{(n,n)} = \mathbf{\Gamma}^{(n,n)} \otimes \mathbf{I} = (\mathbf{L}\mathbf{L}^T) \otimes \mathbf{I} = (\mathbf{L} \otimes \mathbf{I})(\mathbf{L}^T \otimes \mathbf{I}),$$

in which case application of $\mathbf{H}^{(n,n)^{-1}}$ can be applied stably via triangular solve. However, we found that performing

Table I: Cost comparison between dimension tree ALS and Gauss-Newton methods. Depth is quantified with \tilde{O} to omit logarithmic depth factors associated with summations.

method	work	depth
ALS dimension tree [19]	$O(s^N R + NR^3)$	$\tilde{O}(N + R)$
GN with Cholesky [30]	$O(s^N R + N^3 s^3 R^3)$	$\tilde{O}(NsR)$
GN with fast inverse [33]	$O(s^N R + N^3 R^6)$	$\tilde{O}(NR^2)$
GN with faster inverse [44]	$O(s^N R + NR^6)$	$\tilde{O}(R^2)$
Implicit GN CG step [40]	$O(N^2 sR^2)$	$\tilde{O}(1)$
GN step with I CG iter	$O(s^N R + IN^2 sR^2)$	$\tilde{O}(N + R + I)$
GN step with exact CG	$O(s^N R + N^3 s^2 R^3)$	$\tilde{O}(NsR)$

triangular solves via ScaLAPACK [10] is a bottleneck for parallel execution (see the weak scaling results in Section V), as backward and forward substitution have polynomial depth. Consequently, we compute the inverse of $\Gamma^{(n,n)}$ and use tensor contractions to apply it in our parallel implementation.

D. Complexity comparison between ALS and GN

We present the cost of our Gauss-Newton implementation in Table I. The right hand side of the Gauss-Newton iteration is the gradient of the residual function, which can be calculated using dimension trees similar to the ALS algorithm, thus requiring $O(s^N R)$ amount of work, the same as an ALS sweep. With the use of implicit CG to solve the linear least squares problems in Gauss-Newton, the cost can be dominated by CG iterations, each of which requires $O(N^2 sR^2)$ work. In theory, the method should converge in $O(NsR)$ CG iterations.

We contrast this iterative approach to the best known methods for direct inversion of the approximate Hessian for CP decomposition with Gauss-Newton. These approaches exploit the block structure of the approximate Hessian matrix, achieving a cost of $O(N^3 R^6)$ [33], which may be improved to $O(NR^6)$ at the sacrifice of some numerical stability [44]. These methods accelerate inversion when R is small.

However, CP decomposition may be accelerated by an initial Tucker factorization to decrease any dimension greater than R down to R . Tucker preserves exact CP rank and is easier to compute than CP (HoSVD is exact provided existence of an exact Tucker decomposition and is near-optimal for approximation). When $R \geq s$, it is less clear whether the iterative or direct method is preferred. One overhead of the direct approach is a memory footprint overhead of $O(NR^4)$.

We quantify the work and depth (number of operation along critical path, lower bound on parallel cost) of ALS and alternative methods for Gauss-Newton in Table I. The depth analysis for Gauss-Newton with CG assumes use of preconditioning with explicit inverse computation. To quantify the depth of direct linear system solves (necessary in ALS and direct Gauss-Newton), we assume standard approaches (e.g., Gaussian elimination), which have a depth equal to matrix dimension, as opposed to polylogarithmic-depth matrix inversion methods [12]. The communication costs associated with ALS and Gauss-Newton methods can be reduced to known analysis for MTTKRP [7], matrix multiplication [38], and Cholesky factorization [5]. This analysis of cost and depth

suggests that Gauss-Newton with implicit CG achieves the best cost and parallelism among Gauss-Newton variants when $s = O(R)$. However, ALS generally offers more parallelism than Gauss-Newton with implicit CG, when the number of CG iterations is sufficiently large so as to dominate cost.

IV. IMPLEMENTATION

We implement both dimension tree based ALS algorithm and Gauss-Newton algorithm in Python¹. We leverage a backend wrapper for both NumPy and the Python version of Cyclops Tensor Framework [39], so that our code can be tested and efficiently executed both sequentially and with distributed-memory parallelism for tensor operations. In addition, we write both the ALS and Gauss-Newton optimization algorithms in an optimizer class, and each ALS sweep / Gauss-Newton iteration is encapsulated as a step member function in the optimizer class. This framework can be easily extended to included other optimization algorithms for tensor decompositions. Cyclops provides a high-level abstraction for distributed-memory tensors, including arbitrary tensor contractions and matrix factorizations such as Cholesky and SVD via ScaLAPACK [10]. The ALS implementation is based on previous work [22] and uses dimension trees to minimize cost.

Our tensor contraction formulation of the Gauss-Newton method makes it easy to implement with NumPy and Cyclops. Both libraries provide an `einsum` routine for tensor contractions specified in Einstein summation notation. Using this routine, the Gauss-Newton method can be specified succinctly as in the following code snippet, where lists of tensors are used to store the factor matrices $\mathbf{A}^{(n)}$, components of the input and output vector $\mathbf{v}^{(p)}$ and $\mathbf{u}^{(n)}$, and matrices $\Gamma^{(n,p)}$.

```

u = []
for n in range(N):
    u.append(zeros((s, R)))
    for p in range(N):
        if n == p:
            u[n] += einsum("rz,kz->kr", Gamma[n,p], v[p])
        else:
            u[n] += einsum("kz,lr,rz,lz->kr", \
                           A[n], A[p], Gamma[n,p], v[p])

```

Listing 1: Implicit Matrix-Vector Product in GN Method

V. NUMERICAL EXPERIMENTS

We performed numerical experiments to compare the performance of dimension tree based ALS algorithm and Gauss-Newton algorithm on both synthetic and application tensors. Our experiments consider three types of tensors:

Tensors made by random matrices. We create tensors based on known uniformly distributed randomly-generated factor matrices $\mathbf{A}^{(n)} \in (a, b)^{s \times R}$, $\mathcal{X} = [\mathbf{A}^{(1)}, \dots, \mathbf{A}^{(N)}]$.

Quantum chemistry tensors. We also performed CP decomposition on the density fitting intermediate (Cholesky factor of the two-electron integral tensor) arising in quantum chemistry. This CP decomposition yields the tensor hypercontraction

¹Our implementations are publicly available at https://github.com/cyclops-community/tensor_decomposition.

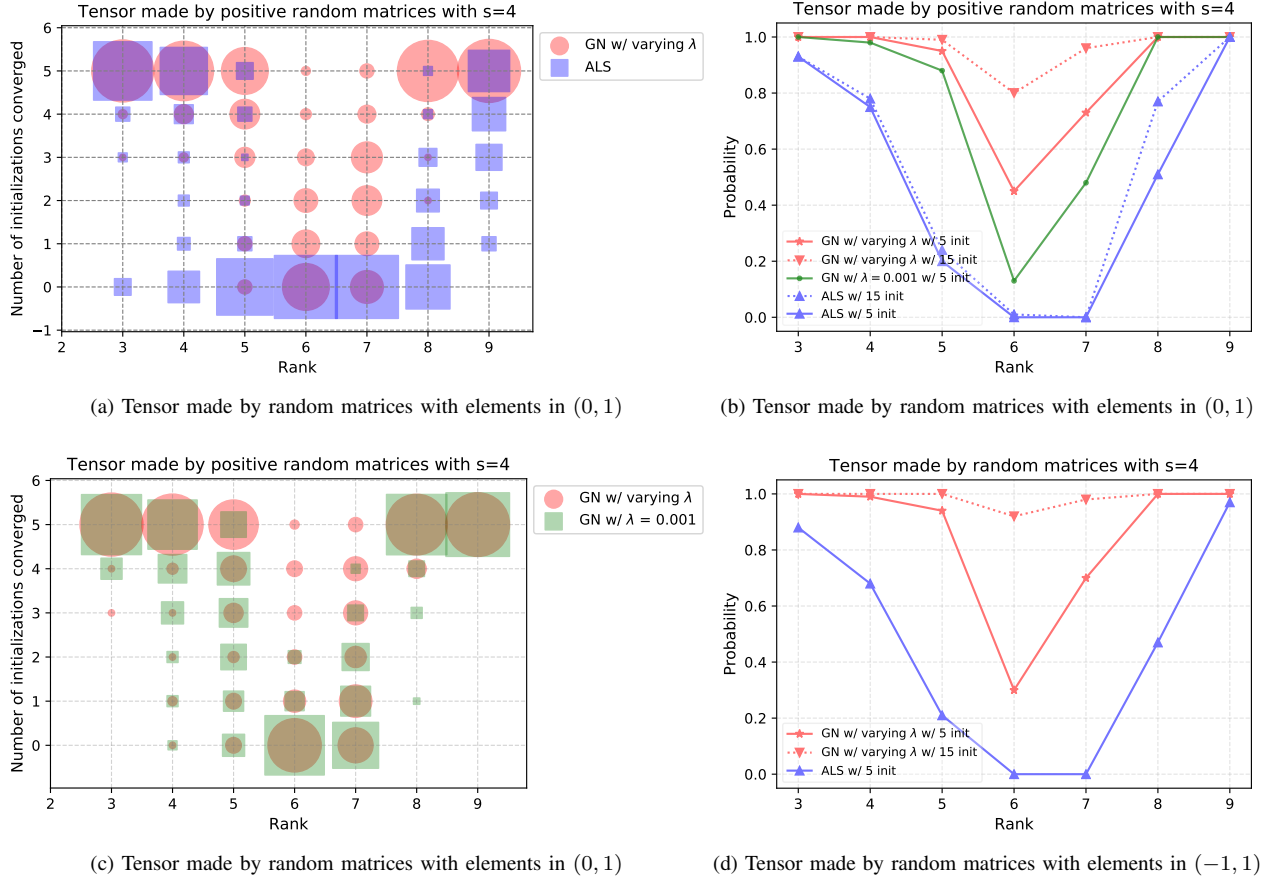


Figure 1: Experimental results for convergence probability of CP decompositions of random low-rank tensors.

format of the two-electron integral tensor, which enables reduced computational complexity for a number of post-Hartree-Fock methods [16]. Acceleration of CP decomposition for this quantity has previously been a subject of study in quantum chemistry [17]. We leverage the PySCF library [42] to generate the three dimensional compressed density fitting tensor, representing the compressed restricted Hartree-Fock wave function of a water molecule chain systems with a STO-3G basis set. We vary the number of molecules in the system from 3 to 40, comparing the efficacy of ALS and Gauss-Newton method under different settings.

Matrix multiplication tensor. A hard case for CP decomposition is the matrix multiplication tensor, defined as an order three unfolding (combining pairs of consecutive modes) of

$$t_{ijklmn} = \delta_{lm}\delta_{ik}\delta_{nj}.$$

This tensor simulates multiplication of matrices A and B via

$$c_{ij} = \sum_{klmn} t_{ijklmn} a_{kl} b_{mn} = \sum_l a_{jl} b_{li}.$$

Its exact CP decompositions give different bilinear algorithms for matrix multiplication, including classical matrix multiplication with rank $s^{3/2}$ and Strassen’s algorithm [41] with rank $s^{\log_4(7)}$. Determining the minimal CP rank for multiplication

of n -by- n matrices with $n \geq 3$ (so $s \geq 9$) is an open problem [31] that is very important in theory and practice.

To maintain consistency throughout the experiments, we run CG till a relative tolerance of 10^{-3} . We use the metrics *relative residual* and *fitness* to evaluate the convergence. Let $\tilde{\mathcal{X}}$ denote the tensor reconstructed by the factor matrices, the relative residual and fitness are defined as follows,

$$r = \frac{\|\mathcal{X} - \tilde{\mathcal{X}}\|_F}{\|\mathcal{X}\|_F}, \quad f = 1 - \frac{\|\mathcal{X} - \tilde{\mathcal{X}}\|_F}{\|\mathcal{X}\|_F}.$$

We collect our experimental results with NumPy backend on the Blue Waters Supercomputer, and our results with Cyclops backend on the Stampede2 supercomputer Texas Advanced Computing Center located at the University of Texas at Austin using XSEDE [47].

On Blue Waters, we use one processor of the XE6 dual-socket nodes for each sequential experiment with NumPy backend. On Stampede2, we leverage the Knight’s Landing (KNL) nodes exclusively, each of which consists of 68 cores, 96 GB of DDR RAM, and 16 GB of MCDRAM. These nodes are connected via a 100 Gb/sec fat-tree Omni-Path interconnect. We use Intel compilers and the MKL library for BLAS and batched BLAS routines within Cyclops. We use 64 processes per node on Stampede2 for all experiments.

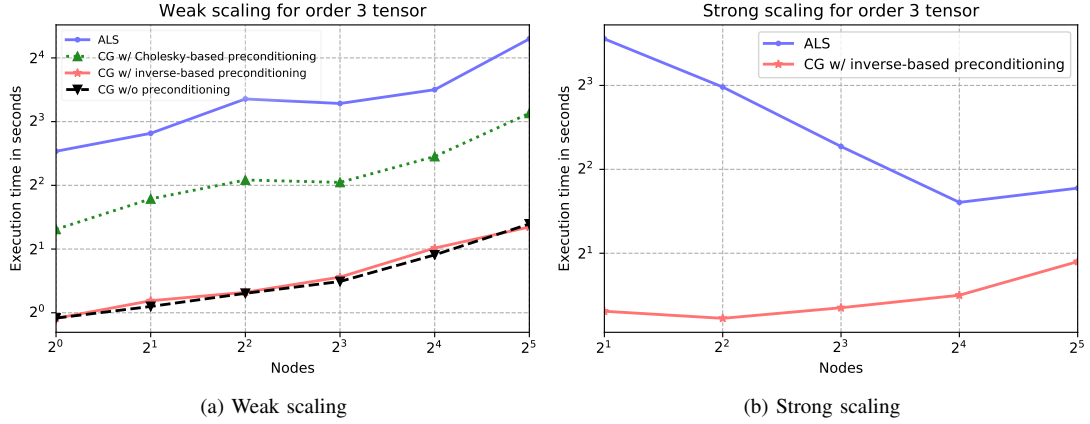


Figure 2: Benchmark results for one ALS sweep vs one CG iteration. Each data point is the mean time across 10 iterations.

We study the effectiveness of ALS and Gauss-Newton on CP decomposition based on the following metrics:

Convergence likelihood. We compare the likelihood of the CP decomposition to recover the original low rank structure of the input tensor with both algorithms.

Convergence behavior. We compare the convergence progress w.r.t. execution time of ALS and Gauss-Newton for all the tensors listed above. Experiments are performed with NumPy backend for small and medium-sized tensors, while the Cypclops backend is used for large tensors.

Parallel Performance. We perform a parallel scaling analysis to compare the simulation time for one ALS sweep of the dimension tree based ALS algorithm and the conjugate gradient iteration of the Gauss-Newton algorithm.

A. Convergence likelihood

We compare the convergence likelihood of CP decomposition for random low-rank tensors, optimized with ALS algorithm and Gauss-Newton algorithm with constant and varying regularization. We run the algorithms until the residual norm is less than 5×10^{-5} , or the norm of the update is less than 10^{-7} , or a maximum of 500 and 10,000 iterations for Gauss-Newton and ALS, respectively. The results are presented in Figure 1. We set the tensor order $N = 3$, size in each dimension $s = 4$, and compare the convergence likelihood under different CP ranks. These results are representative of behavior observed across a variety of choices of s and N .

In Figure 1a, we run Gauss-Newton and ALS on 100 problems with factor matrices sampled from $(0, 1)$ with 5 initializations each for CP rank ranging from 3 to 9. The diameter of the circle and the side length of the square are proportional to the number of problems converged for the corresponding number of initializations. It is evident that Gauss-Newton exhibits a higher probability of convergence than ALS as the circles are always bigger than the squares for higher number of initializations converged. In Figure 1c, we compare Gauss-Newton with varying regularization and constant regularization with $\lambda = 10^{-3}$ for the same set-up.

We observe that Gauss-Newton with varying regularization is more likely to converge to the exact solution as compared to when regularization is constant.

In Figure 1b, we run both algorithms with the same set-up. Each of the points in the plot represents the probability of convergence of the algorithm to the exact solution for at least one out of the respective number of initializations. We observe that Gauss-Newton with the varying regularization method is more likely to converge for ‘hard’ cases, as the probability for rank 6 and 7 is 0.45 and 0.73 respectively with 5 initializations whereas it is 0.13 and 0.48 for constant regularization and negligible for ALS in these cases. Note that the probability increases when we increase the initializations for Gauss-Newton, while for ALS the probability remains almost the same.

In Figure 1d, we compare Gauss-Newton with varying regularization against ALS under the same set-up except that factor matrices are sampled from $(-1, 1)$. We can again observe that Gauss-Newton with varying regularization is more likely to converge and the probability increases as we increase the number of initializations. With the help of these experiments we conclude that Gauss-Newton with varying regularization can lead to better convergence for random tensors.

B. Parallel Performance

We perform a parallel scaling analysis to compare the simulation time for one dimension tree based ALS sweep and one conjugate gradient iteration of the Gauss-Newton algorithm. For weak scaling, on p processors, we consider order $N = 3$ tensors starting with dimension $s = 800$ and rank $R = 800$ and growing both as $p^{1/3}$ with increasing number of nodes p . Figure 2a shows that with the increase of number of nodes, the time for both one ALS sweep and one conjugate gradient iteration increases. This increase is expected, as the amount of work per processor grows as $p^{1/3}$. One conjugate gradient iteration is consistently around 8 times faster than one ALS sweep for different simulation sizes, and both approaches achieve good weak scalability. We observe

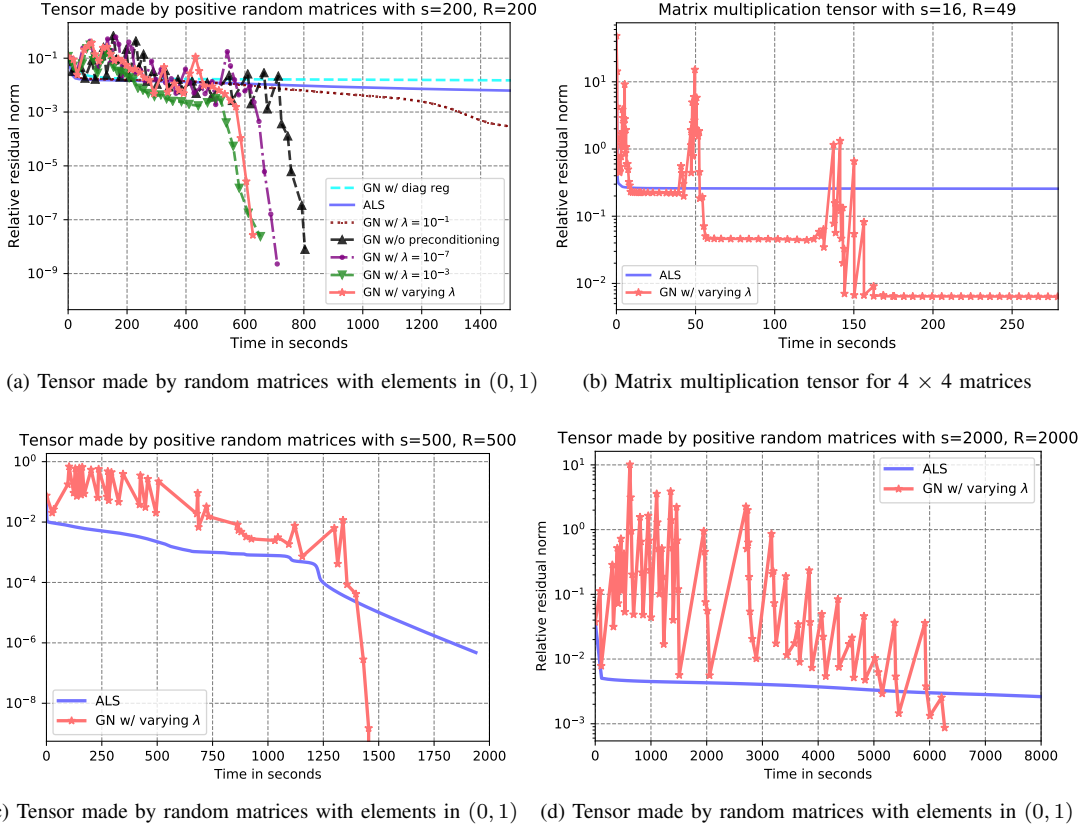


Figure 3: Relative residual norm vs time for the CP decomposition of synthetic tensors with different sizes. The results (a) and (b) are collected with the NumPy backend, while (c) and (d) are collected with the Cyclops backend.

that explicit calculation and use of the inverse eliminates a significant overhead associated with preconditioning using Cholesky and triangular solves.

For strong scaling, we consider order $N = 3$ tensors with dimension size $s = 1200$ and a rank $R = 1200$ CP decomposition. Figure 2b shows that the conjugate gradient iteration time increases with the number of nodes, while the ALS sweep time decreases at first, and increases with more than 16 nodes. The conjugate gradient iteration involves smaller matrix multiplications, and becomes dominated by communication with increasing node counts, thereby slowing down in iteration time. The ALS sweep is dominated by the MTTKRP calculations, which are more easily parallelizable and therefore make ALS achieve better scaling. Overall, we observe that the Gauss-Newton CG iterations contain less parallelism than MTTKRP, but are weakly scalable.

C. Exact CP decomposition

We compare the convergence behavior of different variants of the Gauss-Newton algorithm with ALS for exact (synthetic) CP decomposition in Figure 3. We generate three random low rank tensors of different sizes and a matrix multiplication tensor with $s = 16$. The smaller tensors are tested with NumPy backend and the larger ones with parallel Cyclops backend.

In Figure 3a we use CP decomposition on the random low rank tensors with tensor order $N = 3$, size of each dimension $s = 200$ and CP rank $R = 200$ with NumPy backend. We plot different types of regularization for Gauss-Newton along with ALS to study the convergence behavior and select the best variants of Gauss-Newton to perform further experiments. We observe that Gauss-Newton with varying regularization performs the best and converges to a relative residual norm of 2.69×10^{-8} in 627 seconds, whereas Gauss-Newton with constant regularization with $\lambda = 10^{-3}$, which is the best case among different variants of constant regularization, converges to a relative residual norm of 2.39×10^{-8} by this time. ALS only reaches a relative residual norm of 0.0107 by this time and eventually a relative residual norm of 2×10^{-8} after 22,000 seconds. Also, we observe that Gauss-Newton with $\lambda = 10^{-1}$ and diagonal regularization behave similar to first order methods.

In Figure 3b, we consider the computation of CP decomposition for the matrix multiplication tensor with $s = 16$ and $R = 49$, which would produce Strassen's algorithm. Gauss-Newton method with varying regularization converges to a relative residual norm of 0.0063 in 278 seconds, whereas ALS only reaches a relative residual norm of 0.2567 in 279 seconds. We leave investigations of how to find exact CP

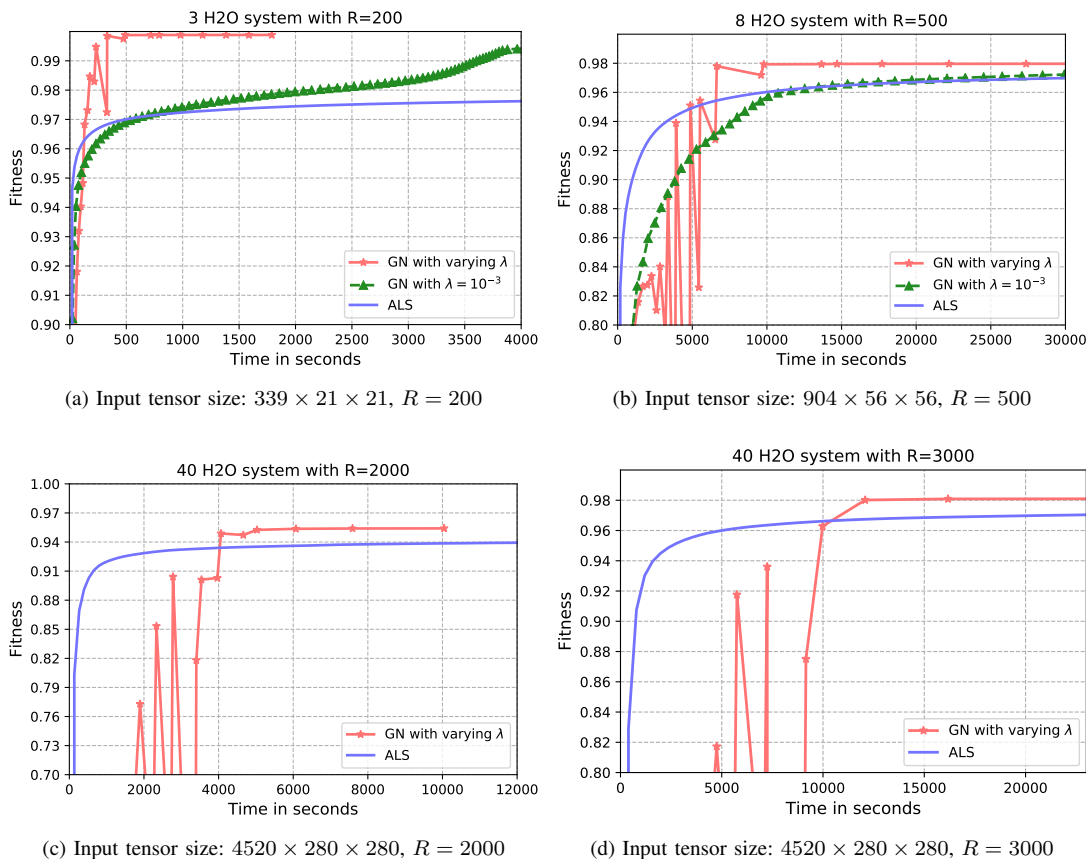


Figure 4: Fitness vs time for the CP decomposition of quantum chemistry tensors with different size and rank. The results (a) and (b) are collected with the NumPy backend, while (c) and (d) are collected with the Cyclops backend.

decompositions of this tensor using specialized techniques [9], [37] for future work.

We test large random low-rank tensors in parallel with $s = 500$, $R = 500$ on 4 nodes with 256 processes as well as $s = 2000$, $R = 2000$ on 16 nodes with 1024 processes using the Cyclops backend. Gauss-Newton with varying regularization outperforms ALS in terms of speed and accuracy in both the cases. For $s = 500$, $R = 500$ as shown in Figure 3c, Gauss-Newton reaches a relative residual norm of 1.5×10^{-9} in 1454 seconds whereas ALS is at 1.5×10^{-9} by this time. For $s = 2000$, $R = 2000$ as shown in Figure 3d, Gauss-Newton with varying regularization reaches a relative residual norm of 0.00086 in 6270 seconds while ALS reaches a relative residual norm of 0.0029 by this time and eventually to 0.0021 in 10,122 seconds. Again, we conclude that Gauss-Newton is a promising algorithm for such problems, despite being somewhat more difficult to parallelize than ALS.

D. Approximate CP decomposition

We also compare the convergence behavior of Gauss-Newton method with ALS for approximate CP decomposition, in which case the tensor reconstructed from factor matrices can only approximate the input tensor rather than fully recover it. We test on the quantum chemistry tensors (density fitting

intermediates). Our results are shown in Figure 4. We test the problem with different input tensor sizes and different CP ranks. We run the two small sized problems shown in Figure 4a, 4b with NumPy backend. We observe that for both problems, Gauss-Newton method outperforms ALS algorithm both in speed and in final fitness. For the 3 water molecules' system, Gauss-Newton reaches the fitness of 0.998 in less than 400 seconds, while the fitness of ALS is less than 0.98 even after 4,000 seconds' running. For the 8 water molecules' system, Gauss-Newton reaches the fitness of 0.979 in less than 10,000 seconds, while the fitness of ALS is less than 0.971 even after 30,000 seconds. In addition, we observe that the Gauss-Newton with our proposed varying regularization scheme outperforms the scheme with constant regularization, as is shown in both figures.

We run the large sized problems set up with 40 water molecules' system shown in Figure 4c, 4d in parallel with Cyclops backend. Results are collected on 4 nodes with total 256 processes on Stampede2. We observe that for these large problems, Gauss-Newton also beats ALS in speed and fitness. With CP rank equals 2,000, Gauss-Newton can reach the fitness of 0.952 in 5,000 seconds, while the best fitness of ALS is less than 0.94 after 12,000 seconds' running. With CP

rank equals 3,000, Gauss-Newton can reach the fitness of 0.98 in 12,000 seconds, while the best fitness of ALS is less than 0.971 after 25,000 seconds of running time.

VI. CONCLUSION

In this paper, we provide the first efficient parallel implementation of a Gauss-Newton method for CP decomposition. We provide a formulation that employs tensor contractions for implicit matrix-vector products within the conjugate gradient method. The use of tensor contractions enables us to employ the Cyclops library for distributed-memory tensor computations to parallelize the Gauss-Newton approach with a high-level Python implementation. Our results demonstrate good weak scalability for the Gauss-Newton method. In addition, we perform extensive experimentation on different kinds of input tensors and compare the convergence and performance of the Gauss-Newton method relative to ALS. We observe that the Gauss-Newton method typically achieves better convergence results than ALS, and we identify a new regularization strategy that performs well across a variety of benchmarks.

VII. ACKNOWLEDGMENTS

Navjot Singh, Linjian Ma, and Edgar Solomonik were supported by the US NSF OAC SSI program, award No. 1931258. This work used the Extreme Science and Engineering Discovery Environment (XSEDE), which is supported by National Science Foundation grant number ACI-1548562. We used XSEDE to employ Stampede2 at the Texas Advanced Computing Center (TACC) through allocation TG-CCR180006. This research is part of the Blue Waters sustained-petascale computing project, which is supported by the National Science Foundation (awards OCI-0725070 and ACI-1238993) and the state of Illinois. Blue Waters is a joint effort of the University of Illinois at Urbana-Champaign and its National Center for Supercomputing Applications.

REFERENCES

- [1] E. Acar, D. M. Dunlavy, and T. G. Kolda. A scalable optimization approach for fitting canonical tensor decompositions. *Journal of Chemometrics*, 25(2):67–86, 2011.
- [2] A. Anandkumar, R. Ge, D. J. Hsu, S. M. Kakade, and M. Telgarsky. Tensor decompositions for learning latent variable models. *Journal of Machine Learning Research*, 15(1):2773–2832, 2014.
- [3] A. Anandkumar, R. Ge, and M. Janzamin. Guaranteed non-orthogonal tensor decomposition via alternating rank-1 updates. *arXiv preprint arXiv:1402.5180*, 2014.
- [4] E. Bailey and S. Aeron. Word embeddings via tensor factorization. *arXiv preprint arXiv:1704.02686*, 2017.
- [5] G. Ballard, J. Demmel, O. Holtz, and O. Schwartz. Communication-optimal parallel and sequential Cholesky decomposition. *SIAM Journal on Scientific Computing*, 32(6):3495–3523, 2010.
- [6] G. Ballard, K. Hayashi, and R. Kannan. Parallel nonnegative CP decomposition of dense tensors. *arXiv preprint arXiv:1806.07985*, 2018.
- [7] G. Ballard, N. Knight, and K. Rouse. Communication lower bounds for matricized tensor times Khatri-Rao product. In *2018 IEEE International Parallel and Distributed Processing Symposium (IPDPS)*, pages 557–567. IEEE, 2018.
- [8] C. Battaglino, G. Ballard, and T. G. Kolda. A practical randomized CP tensor decomposition. *SIAM Journal on Matrix Analysis and Applications*, 39(2):876–901, 2018.
- [9] A. R. Benson and G. Ballard. A framework for practical parallel fast matrix multiplication. In *ACM SIGPLAN Notices*, volume 50, pages 42–53. ACM, 2015.
- [10] L. S. Blackford, J. Choi, A. Cleary, E. D’Azevedo, J. Demmel, I. Dhillon, S. Hammarling, G. Henry, A. Petitet, K. Stanley, D. Walker, and R. C. Whaley. *ScaLAPACK User’s Guide*. Society for Industrial and Applied Mathematics, Philadelphia, PA, USA, 1997.
- [11] F. Cong, Q.-H. Lin, L.-D. Kuang, X.-F. Gong, P. Astikainen, and T. Ristaniemi. Tensor decomposition of EEG signals: A brief review. *Journal of neuroscience methods*, 248:59–69, 2015.
- [12] L. Csanky. Fast parallel matrix inversion algorithms. In *16th Annual Symposium on Foundations of Computer Science (sfcs 1975)*, pages 11–12. IEEE, 1975.
- [13] R. A. Harshman. Foundations of the PARAFAC procedure: models and conditions for an explanatory multimodal factor analysis. 1970.
- [14] K. Hayashi, G. Ballard, J. Jiang, and M. Tobia. Shared memory parallelization of MTTKRP for dense tensors. *arXiv preprint arXiv:1708.08976*, 2017.
- [15] F. L. Hitchcock. The expression of a tensor or a polyadic as a sum of products. *Studies in Applied Mathematics*, 6(1-4):164–189, 1927.
- [16] E. G. Hohenstein, R. M. Parrish, C. D. Sherrill, and T. J. Martínez. Communication: Tensor hypercontraction. III. Least-squares tensor hypercontraction for the determination of correlated wavefunctions. *The Journal of Chemical Physics*, 137(22):221101, 2012.
- [17] F. Hummel, T. Tsatsoulis, and A. Grüneis. Low rank factorization of the Coulomb integrals for periodic coupled cluster theory. *The Journal of chemical physics*, 146(12):124105, 2017.
- [18] L. Karlsson, D. Kressner, and A. Uschmajew. Parallel algorithms for tensor completion in the CP format. *Parallel Computing*, 57:222–234, 2016.
- [19] O. Kaya and B. Uçar. *Parallel CP decomposition of sparse tensors using dimension trees*. PhD thesis, Inria-Research Centre Grenoble–Rhône-Alpes, 2016.
- [20] T. G. Kolda and B. W. Bader. Tensor decompositions and applications. *SIAM review*, 51(3):455–500, 2009.
- [21] N. Li, S. Kindermann, and C. Navasca. Some convergence results on the regularized alternating least-squares method for tensor decomposition. *Linear Algebra and its Applications*, 438(2):796–812, 2013.
- [22] L. Ma and E. Solomonik. Accelerating alternating least squares for tensor decomposition by pairwise perturbation. *arXiv preprint arXiv:1811.10573*, 2018.
- [23] K. Maruhashi, F. Guo, and C. Faloutsos. Multiaspectforensics: Pattern mining on large-scale heterogeneous networks with tensor analysis. In *2011 International Conference on Advances in Social Networks Analysis and Mining*, pages 203–210. IEEE, 2011.
- [24] B. C. Mitchell and D. S. Burdick. Slowly converging PARAFAC sequences: swamps and two-factor degeneracies. *Journal of Chemometrics*, 8(2):155–168, 1994.
- [25] D. Mitchell, N. Ye, and H. De Sterck. Nesterov acceleration of alternating least squares for canonical tensor decomposition. *arXiv preprint arXiv:1810.05846*, 2018.
- [26] J. J. Moré. The Levenberg-Marquardt algorithm: implementation and theory. In *Numerical analysis*, pages 105–116. Springer, 1978.
- [27] K. R. Murphy, C. A. Stedmon, D. Graeber, and R. Bro. Fluorescence spectroscopy and multi-way techniques. PARAFAC. *Analytical Methods*, 5(23):6557–6566, 2013.
- [28] C. Navasca, L. De Lathauwer, and S. Kindermann. Swamp reducing technique for tensor decomposition. In *2008 16th European Signal Processing Conference*, pages 1–5. IEEE, 2008.
- [29] D. Nion and L. De Lathauwer. An enhanced line search scheme for complex-valued tensor decompositions. Application in DS-CDMA. *Signal Processing*, 88(3):749–755, 2008.
- [30] P. Paatero. A weighted non-negative least squares algorithm for three-way PARAFAC factor analysis. *Chemometrics and Intelligent Laboratory Systems*, 38(2):223–242, 1997.
- [31] V. Pan. *How to Multiply Matrices Faster*. Springer-Verlag New York, Inc., New York, NY, USA, 1984.
- [32] A.-H. Phan, P. Tichavský, and A. Cichocki. Fast alternating LS algorithms for high order CANDECOMP/PARAFAC tensor factorizations. *IEEE Transactions on Signal Processing*, 61(19):4834–4846, 2013.
- [33] A.-H. Phan, P. Tichavský, and A. Cichocki. Low complexity damped Gauss-Newton algorithms for CANDECOMP/PARAFAC. *SIAM Journal on Matrix Analysis and Applications*, 34(1):126–147, 2013.
- [34] M. Rajih, P. Comon, and R. A. Harshman. Enhanced line search: A novel method to accelerate PARAFAC. *SIAM journal on matrix analysis and applications*, 30(3):1128–1147, 2008.

- [35] M. D. Schatz, T. M. Low, R. A. van de Geijn, and T. G. Kolda. Exploiting symmetry in tensors for high performance: Multiplication with symmetric tensors. *SIAM Journal on Scientific Computing*, 36(5):C453–C479, 2014.
- [36] N. D. Sidiropoulos, L. De Lathauwer, X. Fu, K. Huang, E. E. Papalexakis, and C. Faloutsos. Tensor decomposition for signal processing and machine learning. *IEEE Transactions on Signal Processing*, 65(13):3551–3582.
- [37] A. Smirnov. The bilinear complexity and practical algorithms for matrix multiplication. *Computational Mathematics and Mathematical Physics*, 53(12):1781–1795, 2013.
- [38] E. Solomonik and J. Demmel. Communication-optimal parallel 2.5D matrix multiplication and LU factorization algorithms. In *European Conference on Parallel Processing*, pages 90–109. Springer, 2011.
- [39] E. Solomonik, D. Matthews, J. R. Hammond, J. F. Stanton, and J. Demmel. A massively parallel tensor contraction framework for coupled-cluster computations. *Journal of Parallel and Distributed Computing*, 74(12):3176–3190, 2014.
- [40] L. Sorber, M. Van Barel, and L. De Lathauwer. Optimization-based algorithms for tensor decompositions: Canonical polyadic decomposition, decomposition in rank- $(l_r, l_r, 1)$ terms, and a new generalization. *SIAM Journal on Optimization*, 23(2):695–720, 2013.
- [41] V. Strassen. Gaussian elimination is not optimal. *Numerische Mathematik*, 13(4):354–356, 1969.
- [42] Q. Sun, T. C. Berkelbach, N. S. Blunt, G. H. Booth, S. Guo, Z. Li, J. Liu, J. D. McClain, E. R. Sayfutyarova, S. Sharma, et al. PySCF: The Python-based simulations of chemistry framework. *Wiley Interdisciplinary Reviews: Computational Molecular Science*, 8(1):e1340, 2018.
- [43] P. S. Thomas and T. Carrington Jr. An intertwined method for making low-rank, sum-of-product basis functions that makes it possible to compute vibrational spectra of molecules with more than 10 atoms. *The Journal of chemical physics*, 146(20):204110, 2017.
- [44] P. Tichavský, A. H. Phan, and A. Cichocki. A further improvement of a fast damped Gauss-Newton algorithm for CANDECOMP-PARAFAC tensor decomposition. In *2013 IEEE International Conference on Acoustics, Speech and Signal Processing*, pages 5964–5968. IEEE, 2013.
- [45] G. Tomasi and R. Bro. PARAFAC and missing values. *Chemometrics and Intelligent Laboratory Systems*, 75(2):163–180, 2005.
- [46] G. Tomasi and R. Bro. A comparison of algorithms for fitting the PARAFAC model. *Computational Statistics & Data Analysis*, 50(7):1700–1734, 2006.
- [47] J. Towns, T. Cockerill, M. Dahan, I. Foster, K. Gaither, A. Grimshaw, V. Hazlewood, S. Lathrop, D. Lifka, G. D. Peterson, R. Roskies, J. Scott, and N. Wilkins-Diehr. XSEDE: Accelerating scientific discovery. *Computing in Science and Engineering*, 16(05):62–74, sep 2014.
- [48] L. R. Tucker. Some mathematical notes on three-mode factor analysis. *Psychometrika*, 31(3):279–311, 1966.
- [49] N. Vannieuwenhoven, K. Meerbergen, and R. Vandebril. Computing the gradient in optimization algorithms for the CP decomposition in constant memory through tensor blocking. *SIAM Journal on Scientific Computing*, 37(3):C415–C438, 2015.